Structure of Strontium Ion-Exchanged ETS-4 Microporous Molecular Sieves

Carola Braunbarth,† Hugh W. Hillhouse,† Sankar Nair, and Michael Tsapatsis*

Department of Chemical Engineering, Goessmann Laboratory, University of Massachusetts, Amherst, Massachusetts 01003

Allen Burton and Raul F. Lobo*

Center for Catalytic Science and Technology, Department of Chemical Engineering, University of Delaware, Newark, Delaware 19716

Richard M. Jacubinas and Steven M. Kuznicki

Engelhard Corporation, Iselin, New Jersey 08830-0770

Received November 9, 1999. Revised Manuscript Received March 8, 2000

The structure of strontium ion-exchanged ETS-4 titanosilicate has been refined from X-ray powder diffraction data and compared to the structure of sodium ETS-4. The framework of ETS-4 is highly faulted in two directions and can be described as an intergrowth of four polymorphs. Despite the faulting, both materials have open 8-ring channels in the *b* direction. Faulting probabilities in the *a* and *c* directions close to 50% allow the structures to be modeled using a superposition of the possible polymorphs for the purposes of Rietveld refinement. While the sodium ions in Na-ETS-4 are found to be distributed over two different cation sites, the ions in Sr-ETS-4 are found close to the same positions with the strontium ions selectively occupying the cation site coordinated to the chain-bridging titanium leaving unexchanged sodium ions in the 6-ring cation site. The chain-bridging titaniums in Sr-ETS-4 were found to be five-coordinated in square-pyramidal polyhedra, as indicated by an occupancy of the apical oxygen of 1.03 oxygens per unit cell and a Ti−O bond distance of 1.75 ±0.04 Å to the apical oxygen. The ideal formula for Sr-ETS-4 was determined to be $NaSr_4Si_{12}Ti_5O_{38}(OH)\cdot 12H_2O$ with lattice constants $a = 23.1962(12)$ Å, $b = 7.23810(33)$ Å, $c = 6.96517(31)$ Å, $\alpha = \beta = \gamma = 90°$ in the *Cmmm* space group. Site ordering of the cations and the presence of five-coordinated titanium may help understanding the recently reported methane/nitrogen gas separation properties of this new molecular sieve.

Introduction

ETS-4 (Engelhard Titano-Silicate-4) belongs to a class of framework titanosilicate microporous molecular sieves that unlike zeolites are built of tetrahedral as well as octahedral (and possibly square pyramidal) units. Like zeolites, ETS-type materials contain channel systems that enable them in principle to be used in the same applications such as adsorption, separation, catalysis, and ion exchange. ETS-4 (here after referred to as Na-ETS-4) was first synthesized in 1990,[1] and since then there have been only a few reports on this molecular sieve.[2−15] Na-ETS-4 has been described as a material of low stability,[3,7−9,12] and no technologically relevant properties have been reported. However, recently a modified form of Na-ETS-4, a heat-treated, strontium ion-exchanged ETS-4 was reported for its use in important and difficult gas separations such as nitrogen/methane and nitrogen/oxygen.[16] Motivated by these results, we have investigated the structure of strontium

* Corresponding authors.
† Authors contributed equally.

(1) Kuznicki, S. M. Preparation of small-pored crystalline titanium molecular sieve zeolites. U.S. Patent 4938939, 1990.
(2) Chapman, D. M.; Roe, A. L. *Zeolites* **1990**, *10*, 730.
(3) Kuznicki, S. M.; Thrush, K. A.; Allen, F. M.; Levine, S. M.; Hamil, M. M.; Hayhurst, D. T.; Mansour, M. Synthesis and adsoptive properties of titanium silicate molecular sieves. In *Molecular Sieves*; Ocelli, M. L., Robson, H. E., Eds.; Nostrand Reinhold: New York, 1992; p 427.
(4) Luca, P. D.; Kuznicki, S. M.; Nastro, A. *Stud. Surf. Sci. Catal.* **1995**, *97*, 443−445.
(5) Nastro, A.; Hayhurst, D. T.; Kuznicki, S. M. *Stud. Surf. Sci. Catal.* **1995**, *98*, 22.
(6) Philippou, A.; Anderson, M. W. *Zeolites* **1996**, *16*, 98−107.
(7) Valtchev, V.; Mintova, S.; Mihailova, B.; Konstantinov, L. *Mater. Res. Bul.* **1996**, *31*, 163−169.
(8) Naderi, M.; Anderson, M. W. *Zeolites* **1996**, *17*, 437−443.
(9) Du, H.; Zhou, F.; Pang, W.; Yue, Y. *Microporous Mater.* **1996**, *7*, 73.
(10) Liu, X.; Thomas, J. K. *Chem. Commun.* **1996**, *12*, 1435−1436.
(11) Mintova, S.; Valtchev, V.; Angelova, S.; Konstantinov, L. *Zeolites* **1997**, *18*, 269−273.
(12) Mihailova, B.; Valtchev, V.; Mintova, S.; Konstantinov, L. *J. Mater. Sci. Lett.* **1997**, *16*, 1303−1304.
(13) Crucianni, G.; Luca, P. D.; Nastro, A.; Pattison, P. *Microporous Mesoporous Mater.* **1998**, *21*, 143−153.
(14) Braunbarth, C. M.; Boudreau, L.; Tsapatsis, M. Accepted for publication in *J. Membr. Sci.*, 2000.
(15) Mihailova, B.; Valtchev, V.; Mintova, S. *Zeolites* **1996**, *16*, 22−24.
(16) (a) Kuznicki, S. M.; Bell, V. A.; Petrovic, I.; Desai, B. T. Small-Pored Crystalline Titanium Molecular Sieve Zeolites and Their Use in Gas Separation Processes. WO9932404A1, 1999. (b) Kuznicki, S. M.; Bell, V. A.; Petrovic, I.; Blosser, P. W. Barium exchanged ETS-4 and its Use in a Process for the Separation of Nitrogen from a Mixture thereof with Methane. WO9932222A1, 1999.

10.1021/cm9907211 CCC: $19.00
Published on Web 06/24/2000

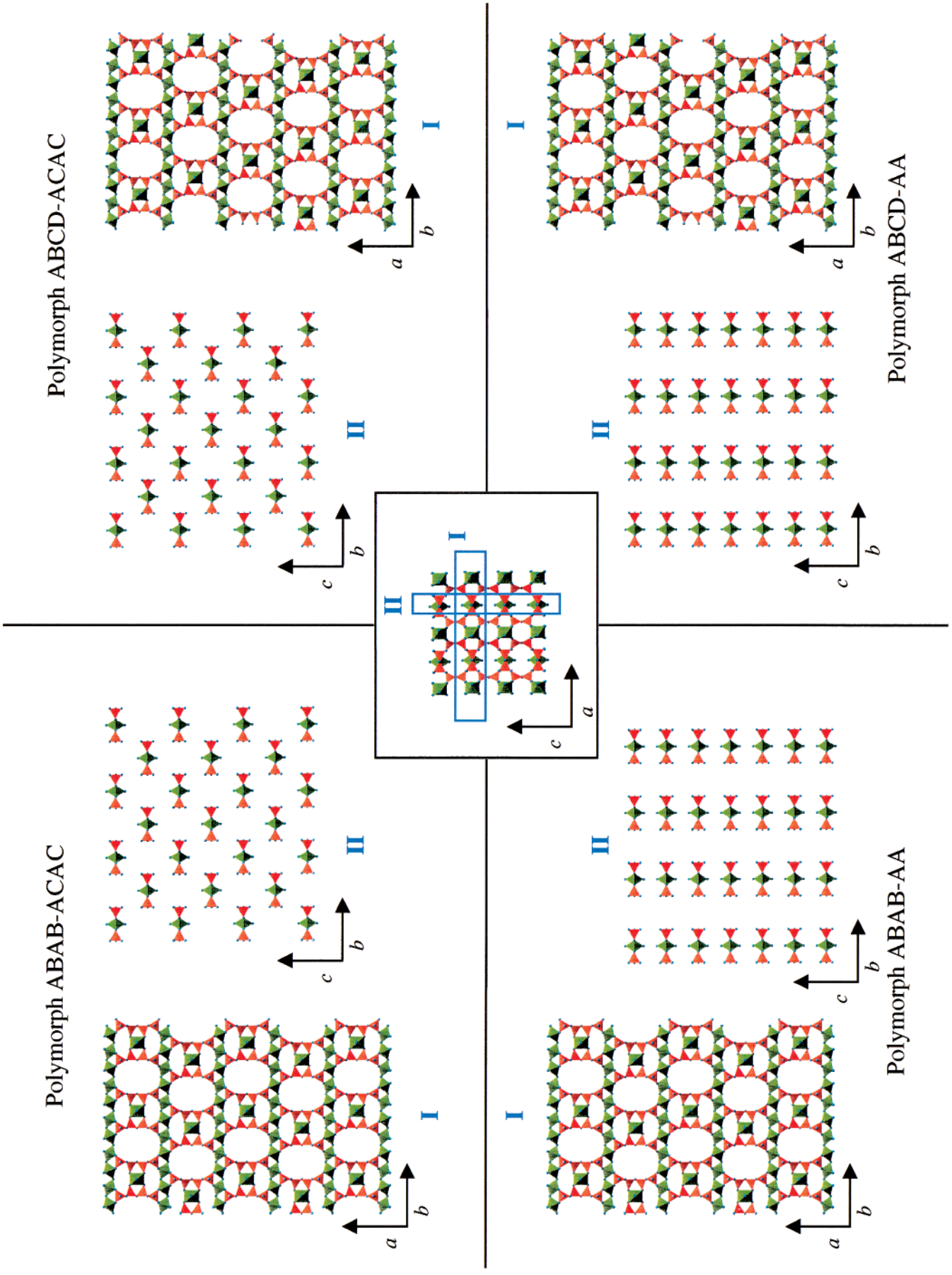
Polymorph ABCD-ACAC
Polymorph ABCD-AA
Polymorph ABAB-ACAC
Polymorph ABAB-AA
I
II
a
b
c

Figure 1. Schematic of the four hypothetical polymorphs of ETS-4 framework. From top left clockwise: Polymorph ABAB-ACAC results from ABAB arrangement along the *a* direction and ACAC arrangement in the *c* direction. Polymorph ABCD-ACAC results from ABCD arrangement along the *a* direction and ACAC arrangement in the *c* direction. Polymorph ABCD-AA results from ABCD arrangement along the *a* direction and AA arrangement in the *c* direction. Polymorph ABAB-AA results from ABAB arrangement along the *a* direction and AA arrangement in the *c* direction. The central scheme represents a view of all polymorphs down the *b* direction along which no faulting takes place. The slices shown in the peripheral schematics are indicated in this central scheme by the boxes.

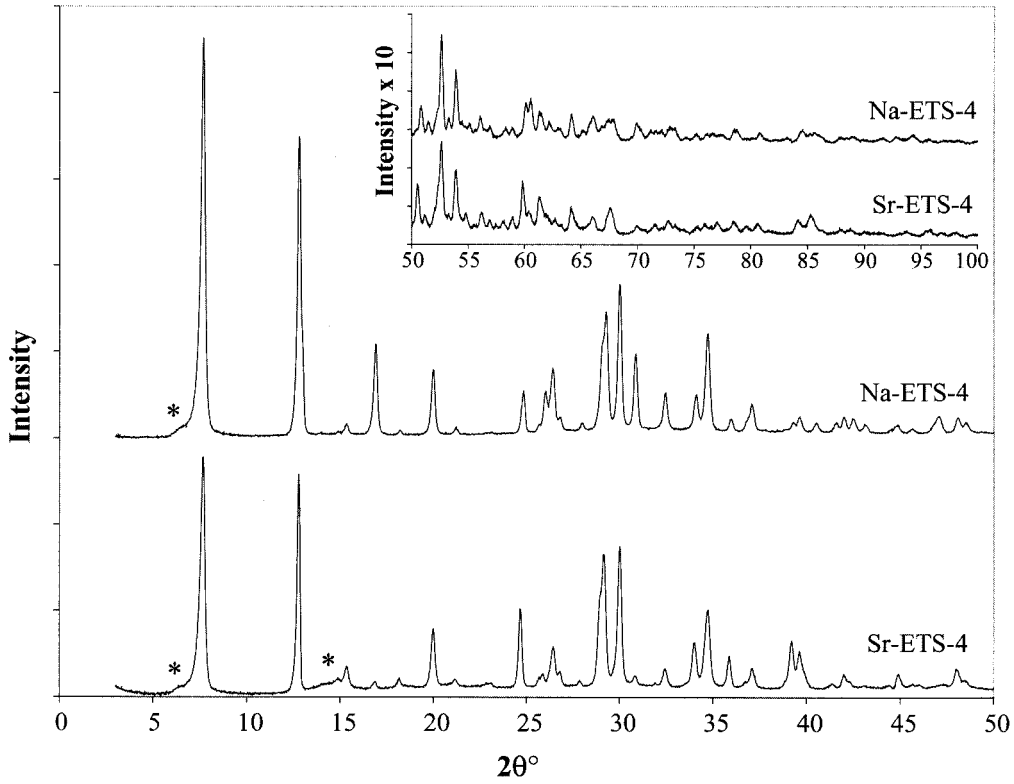

Figure 2. Observed powder X-ray diffraction patterns for as synthesized Na-ETS-4 and Sr-ETS-4. The asterisks mark diffraction peaks not predicted by the superposition model. These peaks have been found to result from small deviations from a completely random sequence of stacking faults.

ion-exchanged ETS-4 (hereafter referred to as Sr-ETS-4), in comparison to Na-ETS-4 which does not show selectivity for the same separations.

The framework of ETS-4 is very similar to the previously reported structure of the mineral zorite[17] and consists of chains of six-coordinated titanium octahedra in the *b* direction. These chains are connected in the *c* direction via a 6-ring and in the *a* direction by either a 12-ring or a bridging titanosilicate unit. The structure of ETS-4 is highly faulted in two directions and can be described as an intergrowth structure of four hypothetical "pure" polymorphs as shown in Figure 1. Two of these polymorphs contain 12-ring pores along the *c* direction (as defined by the unit cell of the *Cmmm* superposition model). One polymorph (monoclinic space group $P112/m$, $a = 12.16$ Å, $b = 14.37$ Å, $c = 13.92$ Å, $\gamma = 107.19°$) consists of an ABCDABCD... (or DCBADCBA...) arrangement of bridging titanosilicate units in the *a* direction[18] while the other polymorph (orthorhombic space group $Pmnm$, $a = 23.23$ Å, $b = 14.37$ Å, $c = 13.92$ Å) consists of an ABAB... arrangement. Upon faulting along the *a* direction, a series of intergrowth structures are formed (similar to those found in ETS-10) which contain sections with both the ABCDABCD... and ABAB... layer arrangements. The amount of each "pure" polymorph in an intergrowth can be described by a simple faulting probability if the distributions of layers is uncorrelated. Another set of polymorphs are obtained by changing the arrangement of bridging units in the *c* direction from AA to AC. The AC arrangement in the *c* direction results in structures defined by monoclinic (space group $A112$, $a = 12.16$ Å, $b = 14.37$ Å, $c = 13.92$ Å, $\gamma = 107.19°$) and orthorhombic (space group $Pmnm$, $a = 23.23$ Å, $b = 14.37$ Å, $c = 13.92$ Å) symmetries corresponding to the ABCD and ABAB arrangements along the *a* direction. Note that any faulting in the AA polymorphs along the *c* direction yields structures with blocked 12-ring pores. However, the faulting in either direction does not block the 8-ring pores in the *b* direction.[6]

Here we report simulations of the faulting patterns with DiFFaX[19,20] that confirm that the faulting probabilities in the *a* and *c* directions of ETS-4 are near 50%. That allows the use of a superposition model, with the *Cmmm* space group, for the refinement of the observed

(17) Sandomirskii, P. A.; Belov, N. V. *Sov. Phys. Crystallogr.* **1979**, *24*, 686−693.

(18) Note that the *c* and *b* lattice constants of these polymorph models are different from the *Cmmm* model used for the Rietveld refinement.

(19) Treacy, M. M. J.; Newsam, J. M.; Deem, M. W. *Proc. R. Soc. London A* **1991**, *443*, 449−520.

(20) Treacy, M. M. J.; Vaughan, D. E. W.; Strohmaier, K. G.; Newsam, J. M. *Proc. R. Soc. London A* **1996**, *452*, 813−840.

diffraction pattern. Cation positions are identified and discussed along with features of the ETS-4 framework.

Experimental Section

Na-ETS-4 was synthesized as previously reported.[1] After crystallization the sample was washed with deionized water until neutral and dried at 90 °C overnight. Titanium(III) chloride (20 wt %, stabilized with HCl, Fisher Scientific) and sodium silicate solution (27 wt % SiO_2, 14 wt % NaOH, Aldrich) were used as titanium and silicon sources, respectively. Sr ion-exchanged ETS-4 was prepared by ion exchange of the as-synthesized Na-ETS-4. The exchange was carried in three steps using aqueous strontium chloride solutions with increasing concentrations (5 wt %, 7.2 wt %, and 8.8 wt % $SrCl_2$). Strontium chloride hexahydrate (99 wt %, Aldrich) was used as the strontium source. In each ion-exchange step the ETS-4 powder was heated in the strontium chloride solution for 1.5 h at 80 °C under reflux, washed twice with boiling deionized water and dried overnight. X-ray diffraction data were collected in a flat-plate geometry from 3° to 100° 2θ with a step size of 0.02° and a counting time of 30 s per step with a Philips X'Pert PW3040 diffractometer using Cu Kα radiation and a graphite monochromator. Inductively-Coupled-Plasma-Mass-Spectrometry (ICP-MS) for chemical analysis was performed by Galbraith Laboratories.

Results and Discussion

The diffraction pattern of Na- and Sr-ETS-4 are given in Figure 2. Figure 3 shows the faulting map of ETS-4 with the pure polymorphs represented at the four corners. The reported simulations that are discussed below include faulting along the *a* and *c* directions as well as combinations of faulting in both directions. The positions of the reported simulations in Figures 4 and 5 are marked with the corresponding numbers for easy reference on this map.

Simulation of X-ray Diffraction Patterns from Faulted Models of ETS-4. Figure 4 shows the results of DiFFaX simulations of powder X-ray diffraction patterns for a sequence of faulted structures. Simulations in each one of the four parts of Figure 4 correspond to structures that lie along the axes of the faulting map of Figure 3. However, none of these one-dimensional faulting simulations yield an entirely satisfactory agreement with the qualitative features of the observed diffraction pattern (Figure 2) between 5° and 16° 2θ. Therefore, diffraction patterns were simulated from structures in the interior regions of the faulting map of Figure 3 by considering faulting in both the *a* and *c* directions simultaneously.

Since DiFFaX can simulate faulting which occurs in only one direction, an approximate scheme was developed to account for the simultaneous faulting in the *a* and *c* directions. Faulting in the *a* direction was approximated by creating supercells composed of 9 unit cells (18 titanosilicate layers) along the *x* axis. Randomly generated numbers were next assigned to the 16 layers which followed the initial two. Each layer was located in either an ABCD... stacking sequence (monoclinic) or ABAB... stacking sequence (orthorhombic) according to the desired overall faulting probability in the *a* direction. For example, in an ~25% monoclinic supercell, the layers associated with the four smallest randomly generated numbers were placed in the supercell in a (local) ABCD sequence while the remaining layers were paced in a stacking order that resembles the orthorhombic polymorph. These supercells were then used in DiFFaX to simulate faulting in the *c* direction.[21] The simulation which yields the best qualitative agreement with the experimental pattern of Sr-ETS-4 is shown in Figure 5. This simulation shows the predicted powder patterns for Sr-ETS-4 structure which contains ~40% of the AA arrangement in the *c* direction and 50% of

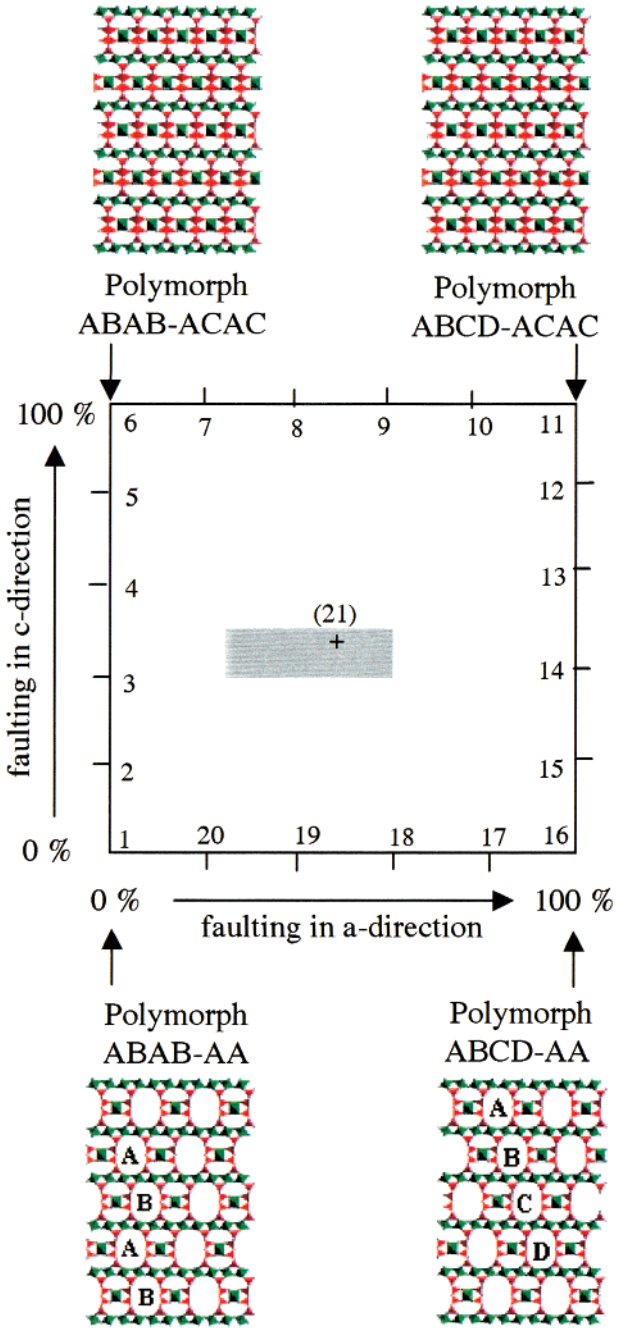

Figure 3. Faulting map for the framework of ETS-4. The numbers correspond to the simulated diffraction patterns shown in Figures 4 and 5. The shaded region indicates the range of faulting probabilities found in Sr-ETS-4.

(21) Eighteen layers were chosen for the supercell because only a limited number of atoms can be used in each layer in the DiFFaX simulations. We tested the effect of changing the specific location of the stacking faults and the effect of different numbers of layers while keeping approximately the same faulting probabilities. We found that these different supercells show virtually identical powder patterns. No appreciable changes could also be observed in supercells with identical ABCD.../ABAB... fractional character but with different assignments of the individual layers.

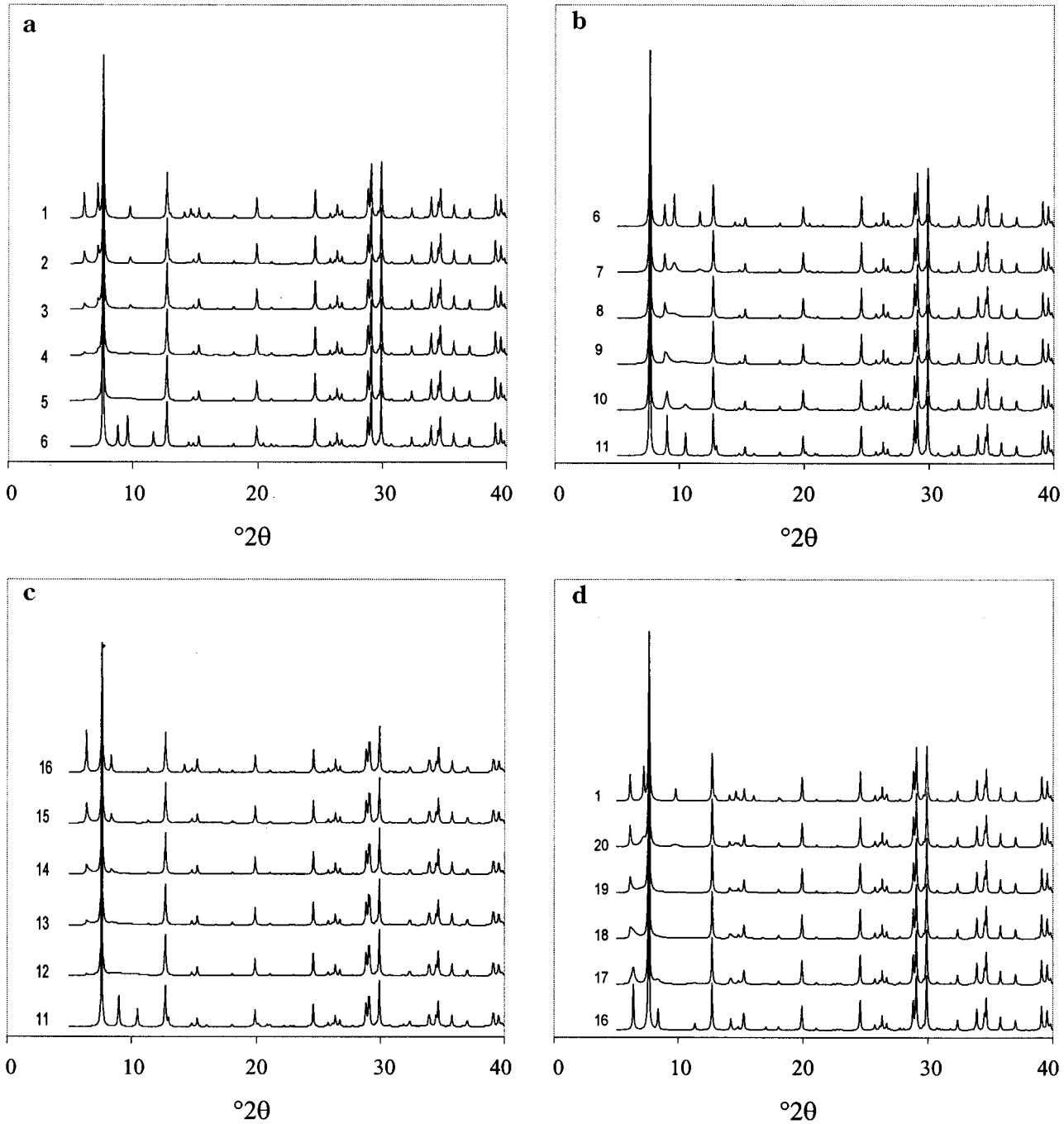

Figure 4. DiFFaX simulations of the powder X-ray diffraction patterns between (a) polymorphs ABAB-AA and ABAB-ACAC, (b) polymorphs ABAB-ACAC and ABCD-ACAC, (c) polymorphs ABCD-ACAC and ABCD-AA, and (d) polymorphs ABCD-AA and ABAB-AA. The numbers indicate the position of the simulated structure on the faulting map of Figure 3.

the ABAB arrangement in the *a* direction. It should be noted that patterns with a fraction of the ABCD (monoclinic) stacking sequence between 25 and 75% in the *a* direction are nearly indistinguishable. On the basis of these simulations, we conclude that the use of a superposition model is a reasonable approximation to the average structure of ETS-4 and that the use of Rietveld method should give a model that allows the understanding of its structure−property relationships.

Rietveld Refinement. The structure of Sr-ETS-4 was refined by the Rietveld method[22] from powder X-ray diffraction data using the GSAS[23] analysis package. The α_2/α_1 ratio was determined from a silicon standard to be 0.5237, and intensities from both Kα peaks were included in the refinement. The structure was refined in the *Cmmm* space group as a superposition of the above discussed polymorphs. This is achieved by allowing the atoms in the bridging titanosilicate unit (Ti2, Si2, etc.) to have fractional occupancies. The diffraction pattern from 16° to 100° 2θ was refined while the low angle region (5° to 16° 2θ) was excluded since the diffraction peaks in this region are very sensitive to the faulting scenario. This approach is justified since the faulting probabilities are close to 50% and the X-ray

(22) Rietveld, H. M. *J. Appl. Crystallogr.* **1969**, *2*, 65−71.

(23) Larson, A. C.; von Dreele, R. B. Report LA UR 86-784, Los Alamos National Lab, 1986.

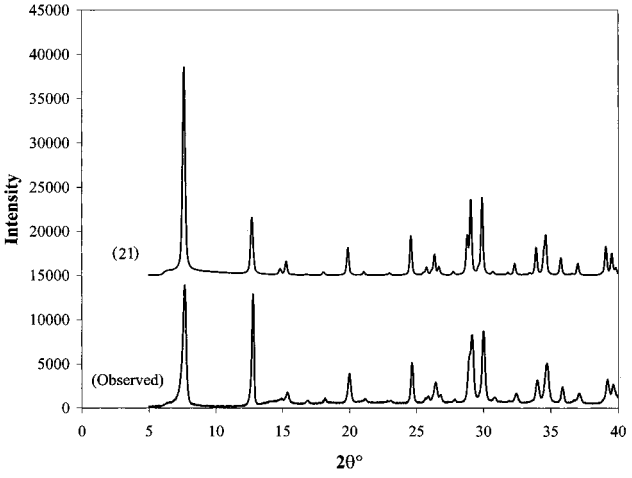

Figure 5. DiFFaX simulation indicating agreement with experimental XRD pattern when faulting in both *a* and *c* directions is included. The number indicates the position of the simulated structure on the faulting map of Figure 3.

pattern is nearly invariant among the polymorphs for angles >16° 2θ. The superposition model does not account for two peaks within this low angle region (see Figure 2). The first is a low intensity peak at 6.5° 2θ (13.6 Å) and the second is a broad peak around 14.5° 2θ (6.1 Å). Analysis of the faulting in this material (see above) indicates that the first peak arises from small deviations from a fully random faulting pattern which cannot be accounted for by the *Cmmm* superposition model used here. The peak around 14.5° 2θ cannot be adequately explained by any of the faulting scenarios investigated. Although this requires further investigation, we currently believe that this could be a small impurity due to a layered phase. However, the refinement is still over-determined since the ratio of the number of reflections to the number of independent atoms is large, and thus, excluding the low-angle region should not affect the accuracy of the refinement.

Previously reported structures of zorite[17] and Na-ETS-4[13] were used as starting points for the current refinement. Soft constraints were applied to Si−O and Ti−O bond lengths, 1.62 and 1.97 Å, respectively, except for the apical oxygen of the bridging titanium position (Ti2) since this bond length helps elucidate the geometry and coordination of the Ti2 site. Also, the occupancies of Ti2, Si2, O5, O6, and O7 were refined subject to a stoichiometric constraint (1 Ti2:4 Si2:2 O5:4 O6:1 O7) in order to model the channel coalescing defects, observed in ETS-10,[24] due to the absence of the [$TiO{\cdot}O_4$-(Si_4O_2)] bridging unit. The occupancy of the apical oxygen (O7) was refined freely on alternating cycles, without the stoichiometric constraint, to elucidate the coordination of the Ti2 site. All soft constraints were released in the final refinement cycles whereupon the model converged to the agreement values shown in Table 1. The final lattice constants, atomic positions, selected bond distances, and bond angles are presented in Tables 2 and 3. The corresponding fit of the X-ray diffraction pattern is shown in Figure 6.

The refined occupancies are supported by chemical analysis as determined by ICP-MS, shown in Table 4,

Table 1. Refinement Parameters for a Polymorph Superposition Model of Sr Ion-Exchanged ETS-4 Titanosilicate[a]

no. of variables	50
no. of observations	4218
no. of reflections	397
no. of background coefficients (shifted Chebyshev polynomial)	10
preferred orientation ratio (*c* axis)	0.978
profile coefficients	
GU, GV, GW	1.0, −1.0, 30.20
LX, LY, ASYM	2.16, 32.26, 7.05
all other coefficients	0
residual index, Rp [%]	5.30
weighted residual, wRp [%]	6.97
reduced χ^2	3.63

[a] A preferred orientation parameter was included based on the March−Dollase model,[28] and peak profiles were modeled using a pseudo-Voigt function incorporating peak asymmetry.[29,30]

and result in a framework that is charge balanced. A small difference was observed in the measured and refined number of silicon atoms and may be accounted for by the presence of a small amount of amorphous silica. One shortcoming of the refinement is the low sensitivity to water−Na^+ replacement due to the fact that they have the same number of electrons and only differ in the shape of the scattering curve.

Structure of Sr-ETS-4. The titanosilicate framework of the Sr-ETS-4 was found to be most similar to the structure of the mineral zorite.[17] The cation sites in Sr-ETS-4 are located close to the cation sites reported for Na-ETS-4;[13] however, an ordering of the cations is observed for the strontium form. The strontium ions are found to selectively occupy the cation site coordinated to both the chain and chain-bridging titanium polyhedra, see Figure 7. The multiplicity of this cation site is 8; however, the maximum theoretical occupancy is 4 due to the proximity of this site generated by symmetry across the mirror plane. As a result the maximum number of strontiums that may be exchanged into the unit cell is 4. The framework charge is balanced by remaining sodium cations found coordinated in the 6-ring between titanium chains. The resulting ideal formula for strontium exchanged ETS-4 is $NaSr_4Si_{12}Ti_5O_{38}(OH){\cdot}12H_2O$, not including defects discussed below. The hypothesis of site ordering of the Sr^{2+} cations was tested by redistributing the cations between both sites and carrying the refinement to completion. These cases always resulted in a higher residual index.

It should be noted that the structure depicted in Figure 7 is of the superposition model, and as such, statistically over half of the strontium cations, Ti2 pyramids, and Si2 tetrahedra shown are absent in the structure. To say more specifically which ones will be absent requires a more detailed understanding of the faulting. We can conclude that at most only one of two adjacent Ti2 sites in the *b* direction is occupied since the Si2 site is four-coordinated. It is also noted that the superposition model cannot distinguish if strontium is present when the chain-bridging titanium is present versus when chain-bridging titanium is absent. However, it appears favorable for the strontium cations to be present when Ti2 is also present due to the favorable environment of that site, coordinated to the oxygens (O3, O4, and O6) of both titanium units at ∼2.65 Å.

Investigating the coordination environment of the chain-bridging titanium in Sr-ETS-4, the refinement

(24) Anderson, M. W.; Terasaki, O.; Ohsuna, T.; Philippou, A.; Mackay, S. P.; Ferreira, A.; Rocha, J.; Lidin, S. *Nature* **1994**, *367*, 347−351.

Table 2. Atomic Parameters for the Superposition Model of Sr Ion-Exchanged ETS-4 in Space Group *Cmmm* with Lattice Constants $a = 23.1962(12)$ Å, $b = 7.23810(33)$ Å, $c = 6.96517(31)$ Å, $\alpha = \beta = \gamma = 90°$

name	*x*	*y*	*z*	occupancy	multiplicity	$U_{iso} \times 10^2$
Ti1	0.25	0.25	0.00	1.00	4	1.11
Ti2	0.00	0.50	0.0433(22)	0.237(3)	4	1.00
Si1	0.16169(14)	0.00	0.2701(5)	1.00	8	1.23
Si2	0.06539(29)	0.0957(9)	0.00	0.475(5)	8	1.41
Na	0.25	0.25	0.50	0.160(11)	4	7.46
Sr	0.36416(12)	0.00	0.2365(4)	0.483(2)	8	1.94
O1	0.15377(41)	0.00	0.50	1.00	4	1.10
O2	0.09785(29)	0.00	0.1851(9)	1.00	8	1.10
O3	0.19627(21)	0.1857(5)	0.2058(7)	1.00	16	1.10
O4	0.21787(39)	0.50	0.00	1.00	4	1.10
O5	0.00	0.00	0.00	0.950(10)	2	1.10
O6	0.06616(45)	0.3228(14)	0.00	0.475(5)	8	1.10
O7	0.00	0.50	0.2915(52)	0.258(3)	4	1.10
Ow1	0.29632(49)	0.0255(39)	0.50	0.50	8	3.44
Ow2	0.09769(178)	0.3689(46)	0.50	0.296(17)	8	12.38
Ow3	0.05381(91)	0.2909(30)	0.50	0.50	8	10.91
Ow4	0.02877(127)	0.00	0.50	0.283(13)	4	2.04

Table 3. Bond Distances (Å) and Angles (Deg) from the Refinement of Sr Ion-Exchanged ETS-4

Ti1 Octahedron		Ti2 Square-Pyramid	
Ti1−O3 [×4]	1.956(5)	Ti2−O6 [×4]	2.023(10)
Ti1−O4 [×2]	1.957(3)	Ti2−O7	1.750(40)
mean	1.96		
O3−Ti1−O3 [×2]	94.25(29)	O6−Ti2−O6 [×2]	98.70(80)
O3−Ti1−O3 [×2]	85.17(29)	O6−Ti2−O6 [×2]	78.70(80)
O3−Ti1−O4 [×4]	88.71(20)	O6−Ti2−O7 [×4]	98.60(270)
O3−Ti1−O4 [×4]	91.29(20)		
mean	90.0		
Si1 Tetrahedron		**Si2 Tetrahedron**	
Si1−O1	1.612(4)	Si2−O2 [×2]	1.646(6)
Si1−O2	1.595(7)	Si2−O5	1.668(7)
Si1−O3 [×2]	1.628(4)	Si2−O6	1.644(12)
mean	1.62	mean	1.65
O1−Si1−O2	105.30(40)	O2−Si2−O2	103.10(60)
O1−Si1−O3 [×2]	109.26(28)	O2−Si2−O5 [×2]	104.00(40)
O2−Si1−O3 [×2]	110.80(25)	O2−Si2−O6 [×2]	114.60(40)
O3−Si1−O3	111.30(40)	O5−Si2−O6	115.20(60)
mean	109.5	mean	109.2
Na1 Environment		**Sr2 Environment**	
Na−O1 [×2]	2.874(7)	Sr−O3 [×2]	2.681(5)
Na−O3 [×4]	2.443(5)	Sr−O4	2.517(7)
Na−Ow1 [×2]	2.265(23)	Sr−O6 [×2]	2.640(11)
		Sr−Ow1	2.425(7)
		Sr−Ow2	2.248(20)

Table 4. Chemical Composition of Sr Ion-Exchanged ETS-4 As Determined by Inductively Coupled Plasma Emission Spectroscopy[a]

atom	no. from formula	no. from refinement	measured no.	± no. at 95% confidence
Si	12	11.80	12.57	0.92
Ti	5	4.95	4.88	0.26
Na	1	0.64	0.65	0.05
Sr	4	3.86	3.95	0.16
O	39	38.73		
O_{water}	12	11.50		

[a] Confidence intervals are shown for the measured values.

converged to an occupancy of 1.03 apical oxygens (O7) per unit cell with Ti−O bond distance of 1.75 ±0.04 Å for the apical oxygen, without using soft restraints, and 2.023 ±0.010 Å for the pyramid base oxygens. Both data suggest the presence of five-coordinated Ti^{4+} with a square-pyramidal geometry. Previously, short Ti−O bond distances have been reported from 1.66 to 1.79 Å for the apical oxygen of this polyhedron[25] with longer bond lengths to the base oxygens. The polyhedron in the current structure is slightly distorted with an aspect ratio of 1.2 for the base of the pyramid. Also, the difference map generated from the structure is featureless to ±0.1 e/Å^3 in the vicinity of the apical oxygen—further supporting the validity of the refined occupancy and position. To date, only one synthetic titanosilicate material has been documented as having five-coordinated titanium.[26] This material, JDF-L1, is a layered barium titanosilicate showing high selectivity for phenol to quinone conversions, owing to the five-coordinated titanium environment. Our results indicate the possibility that ETS-4 is a synthetic framework molecular sieve with five-coordinated titanium. Sandomirskii and Belov[17] first suggested the square-pyramidal structure of the bridging titanium in zorite. However, a recent refinement[13] of Na-ETS-4 indicated that a six-coordinated full octahedron was present at the chain-bridging titanium site. The latter result may be questionable due to very short cation separation distances in the reported structure. The occupancy of the sodium site in question is greater than 50%, and the resulting Na−Na coordination distance of 2.96 Å across the mirror plane cannot be interpreted as an artifact of the superposition model in which one of the sites is vacant. While the current refinement supports the presence of five-coordinated titanium, the coordination environment of the chain-bridging titanium needs further investigation and might be elucidated by EXAFS analysis.

Previous work on the structure of ETS-10[24,27] showed channel-coalescence defects observed in HRTEM images where the bridging titanium was absent resulting in an enlarged opening in the *a*−*b* plane. The possible presence of this type of defect was accounted for in the current refinement by allowing the occupancy of the bridging titanium unit to refine collectively with a stoichiometric constraint. The results indicate that the

(25) Clark, R. J. H. *The Chemistry of Titanium, Zirconium, and Hafnium*; Pergamon Press: New York, 1973.
(26) Roberts, M. A.; Sankar, G.; Thomas, J. M.; Jones, R. H.; Du, H.; Chen, J.; Pang, W.; Xu, R. *Nature* **1996**, *381*, 401−404.
(27) Anderson, M. W.; Terasaki, O.; Ohsuna, T.; Malley, P. J. O.; Philippou, A.; Mackay, S. P.; Ferreira, A.; Rocha, J.; Lidin, S. *Philos. Mag. B* **1995**, *71*, 813−841.
(28) Dollase, W. A. *J. Appl. Crystallogr.* **1986**, *19*, 267−272.
(29) Howard, C. J. *J. Appl. Crystallogr.* **1982**, *15*, 615−620.
(30) Thompson, P.; Cox, D. E.; Hastings, J. B. *J. Appl. Crystallogr.* **1987**, *20*.

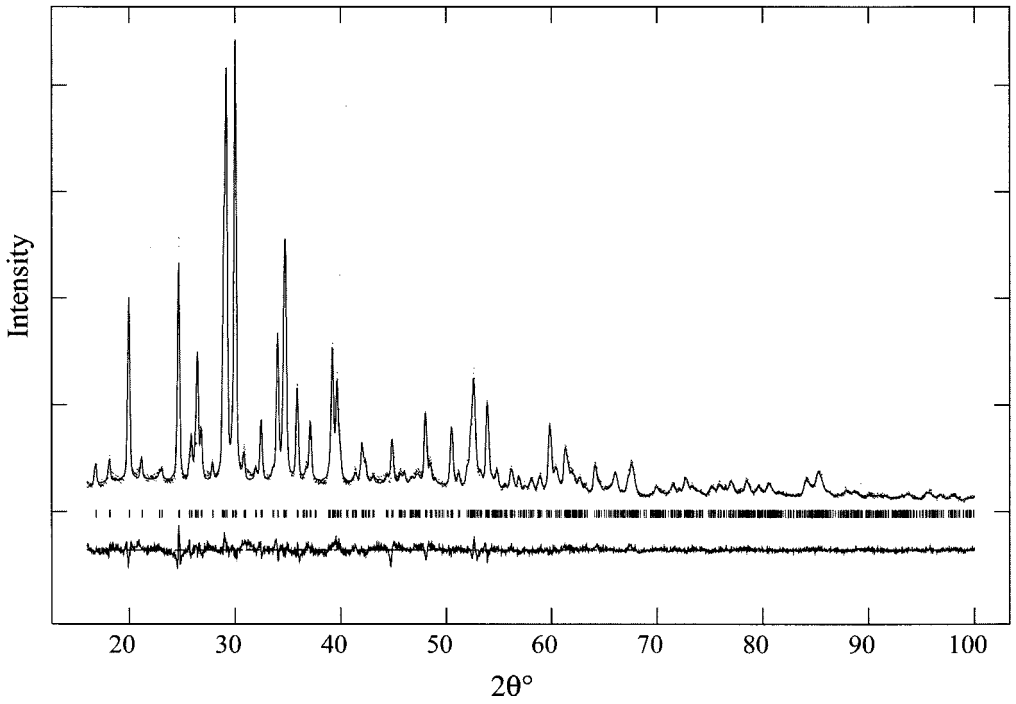

Figure 6. Calculated diffraction pattern from the Rietveld refinement of Sr-ETS-4. The observed data are shown as points with the position of the Bragg reflections and difference between calculated and observed intensities shown below.

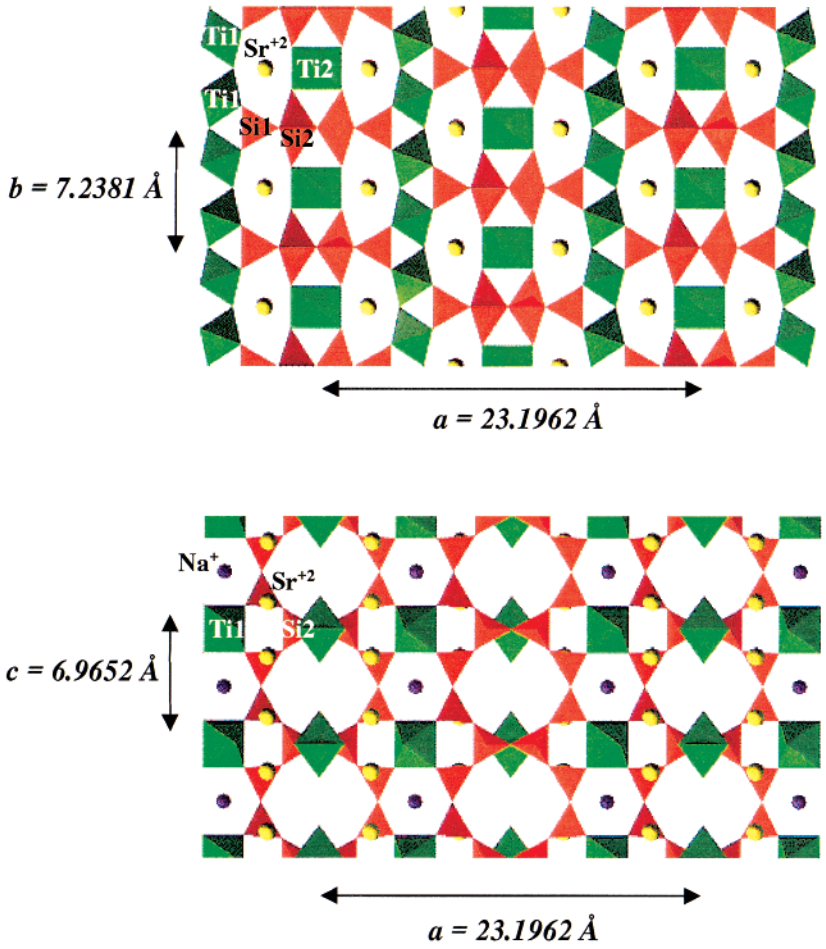

Figure 7. The *a*−*b* and *a*−*c* planes of the *superposition* model of Sr-ETS-4 showing the site ordering of the cations. Note that statistically 85% of the sodium cations, and over half of the strontium cations, Ti2 pyramids (green), and Si2 tetrahedra (red) shown are absent in the structure. Also, the Ti2 sites are shown as bi-pyramidal units; however the O7 site has an occupancy of 0.258. Therefore, since half the Ti2 sites are vacant, statistically only one vertex is occupied when the Ti2 is present. Water not shown for clarity.

bridging titanium unit is present in 47.4% of the unit cells of the superposition model as compared to a theoretical full occupancy of 50%. However this technique is only approximate and yields a conservative estimate of the defect frequency of 5.2% since in the absence of the Ti2 unit there may be cations and/or water at the vacant titanium position.

Conclusions

As synthesized sodium ETS-4 was ion exchanged with strontium to a level of 93%, with respect to the number of sodium ions. Structure refinement of Sr-ETS-4 from X-ray diffraction data indicates that Sr^{2+} preferentially occupies one of the two cation sites that are occupied by sodium in Na-ETS-4. The refinement also indicates that five-coordinated titanium is present in the structure.

Acknowledgment. We gratefully acknowledge and thank Dr. M. Treacy for providing the modified code of DiFFaX allowing the 2D faulting simulations that we used in this work. Funding from Engelhard Co. is gratefully acknowledged. M.T. acknowledges additional support from NSF (CAREER CTS-9624613 and ARI CTS-9512485), the David and Lucile Packard Foundation, and the Camille and Henry Dreyfus Foundation. We also thank Jon Hanson from Brookhaven National Laboratory for general advice on refining crystal structures.

CM9907211